samples from different sources and upon cycling repeatedly through the melting point. These are strong indications against ascribing the layer to surface-active contaminants (*10, 14*). The x-ray measurements (Fig. 2B) (*10*), which show a sharply defined layer of uniform thickness closely correlated with *n*, virtually exclude the possibility of contaminants of lengths significantly different from *n*.

18. B. Berge, L. Faucheux, K. Schwab, A. Libchaber, *Nature* **350**, 322 (1991).
19. C. A. Croxton, *Statistical Mechanics of the Liquid Surface* (Wiley, New York, 1980). With the lack of x-ray or neutron measurements, no clear structural evidence is available for the proposed layering. Furthermore, the in-plane order in the postulated layers, if any, is not known. Reference to these effects in liquid metals as surface freezing is therefore premature at present.
20. J. Timmermans, *Physico-Chemical Constants of Pure Organic Compounds* (Elsevier, New York, 1965); C. I. Poser and I. C. Sanchez, *J. Colloid Interface Sci.* **69**, 539 (1979).
21. P.-G. de Gennes, *Scaling Concepts in Polymer Physics* (Cornell Univ. Press, Ithaca, NY, 1979).
22. X. Z. Wu, E. B. Sirota, S. K. Sinha, B. M. Ocko, M. Deutsch, in preparation.
23. D. G. Legrand and G. L. Gains, Jr., *J. Colloid Interface Sci.* **31**, 162 (1969); D. N. Theodorou, *Macromolecules* **22**, 4578 (1989).
24. J. N. Israelachvili, *Intermolecular and Surface Forces* (Academic Press, Orlando, FL, 1985); J. Mahanty and B. W. Ninham, *Dispersion Forces* (Academic Press, New York, 1976).
25. D. E. Moncton, R. Pindak, S. C. Davey, *Phys. Rev. Lett.* **49**, 1865 (1982); E. B. Sirota, P. S. Pershan, S. Amador, L. B. Sorensen, *Phys. Rev. A* **35**, 2283 (1987); B. D. Swanson, H. Straiger, D. J. Tweet, L. B. Sorensen, *Phys. Rev. Lett.* **62**, 909 (1989); R. Holyst, *Phys. Rev. A* **44**, 3692 (1991).
26. Supported by The U.S.–Israel Binational Science Foundation, Jerusalem (M.D.). Brookhaven National Laboratory is supported by the Division of Materials Research, U.S. Department of Energy under contract DE-AC02-76CH00016.

1 April 1993; accepted 22 June 1993

Giant Magnetoresistance at Low Fields in Discontinuous NiFe-Ag Multilayer Thin Films

T. L. Hylton, K. R. Coffey, M. A. Parker, J. K. Howard

A series of sputtered multilayers of $Ni_{80}Fe_{20}$-Ag was prepared to examine the giant magnetoresistance effect before and after annealing. For a wide range of NiFe and Ag thicknesses, no giant magnetoresistance was observed in the unannealed films. After annealing, a large, negative magnetoresistance was observed of order 4 to 6% in applied fields of order 5 to 10 oersteds at room temperature. The appearance of giant magnetoresistance is concurrent with the breakup of the NiFe layers, which is attributable to a magnetostatic interaction that favors local antiparallel alignment of the moments in adjacent layers. These structures may be of significant practical importance as sensors that require large changes in resistance at low fields, such as magnetoresistive heads used in magnetic recording systems.

Since the discovery of giant magnetoresistance (GMR) in Fe-Cr sandwiches (*1, 2*), GMR has been observed in a variety of magnetic-nonmagnetic multilayer (*3, 4*) and granular alloy systems (*5–7*). The smallest values of resistance are observed in these systems when the magnetization of neighboring layers or clusters is aligned by an applied field, and larger values of resistance are observed when neighboring layers are antialigned or neighboring clusters are "randomly" aligned. With the exception of the spin-valve devices (*4*) and related devices (*8, 9*), the fields necessary to achieve magnetic saturation and a significant magnetoresistive effect are generally too large to make these devices promising in low-field sensor applications. For many multilayer systems, the magnitude and sign of the interlayer exchange coupling is a strong function of the nonmagnetic layer thickness (*10*), which can lead to difficulties in the preparation of the weakly antiferromagnetically coupled structures necessary for low-field sensitivity. For alloy systems, the particle size, shape, and temperature dominate the field dependence of the GMR with the result that low-field sensitivity is not possible in realistic alloy systems (*11*).

We prepared discontinuous multilayers by annealing sputtered multilayers of $Ni_{80}Fe_{20}$-Ag. We postulate that this structure minimizes the effects of crystal and shape anisotropy, providing a magnetostatically induced, antiparallel coupling between layers. As these samples exhibit 4 to 6% GMR at room temperature in fields of 5 to 10 Oe, they satisfy two important criteria in the design of magnetoresistive sensors for magnetic recording heads: a magnetoresistance greater than 2% and a sensitivity greater than 0.5% per oersted. Other equally important criteria, such as noise, durability, and manufacturability, may or may not be satisfied and are the subject of ongoing efforts.

The original motivation for this work is our own theoretical (*11*) and experimental work on GMR in granular alloys of Co-Cu and NiFe-Ag (*12*) and granular, evaporated bilayers of Cu-NiFe and Cu-Co (*13*). The large fields (typically 10 kOe in alloys and 1 kOe in bilayers) necessary to achieve significant GMR in these granular alloys can be attributed to three effects: (i) The typical particle sizes in these systems (20 to 40 Å) are so small that thermal fluctuations easily disorient the particles at a nominal 10-Oe applied field, which we define as "low"; (ii) the anisotropy fields induced by departures in shape of only a few percent from perfect spheres can be large compared with 10 Oe; and (iii) crystalline anisotropy fields are expected to be large compared with 10 Oe in all but the softest alloys, such as $Ni_{80}Fe_{20}$.

The second consideration suggests that greater low-field sensitivity can be achieved if the collection of particles can be given a flat, disk-like shape and oriented such that all the particle surfaces are parallel to the applied field. The in-plane anisotropy induced by departures from a perfectly circular perimeter will be much smaller than in the case of similarly misshapen spherical particles. In an effort to achieve such a structure, we prepared annealed multilayers of immiscible magnetic (NiFe) and nonmagnetic materials (Ag). Under appropriate annealing conditions, we expect penetration of the nonmagnetic material at the grain boundaries of the magnetic layer. Although this may or may not result in a collection of flat, island-like magnetic particles, it will certainly promote a multidomain state within the magnetic layers. These discontinuous multilayers should show properties similar to both continuous multilayers and granular alloys. We chose the NiFe-Ag system because we desired a low anisotropy magnetic alloy and an immiscible spacer material.

The multilayers were prepared by S-gun magnetron sputtering in a mixture of 4% H_2 and 96% Ar at a pressure of 3 mtorr with substrates at ambient temperature. Substrates were 1-inch Si wafers with a thermally grown oxide surface 700 Å thick. A typical sample with n layers of NiFe of thickness x and Ag of thickness y is given by Ta(100 Å)-Ag(y/2)-[NiFe(x)-Ag(y)]$_{n-1}$-NiFe(x)-Ag(y/2)-Ta(40 Å)-SiO_2(700 Å)-Si. A magnetic field of approximately 150 Oe, applied during deposition, resulted in a weak uniaxial anisotropy field of 2 to 3 Oe with significant dispersion. After deposition, the samples were broken into strips of about 8 mm by 1.5 mm and were annealed at atmospheric pressure in a mixture of 5% H_2 and 95% Ar in a rapid thermal processing oven at a variety of temperatures for 10 min. Magnetoresistance measurements were performed with a four-point, in-line geometry of the contacts with the magnetic field applied parallel to the plane of the sample and either perpendicular or parallel to the current direction. Magnetization measurements

IBM ADSTAR, San Jose, CA 95193.

were performed with a vibrating sample magnetometer. In the figures that follow, all measurements were made at room temperature with the applied field parallel to the easy axis (the preferred axis of orientation of the magnetization). Similar results have been obtained on samples with no significant uniaxial anisotropy deposited in the absence of an applied field.

In the range of layer thicknesses examined, 15 to 25 Å for NiFe and 10 to 40 Å for Ag, no significant GMR was observed before the annealing. After annealing, samples achieve GMR magnitudes of typically $\Delta R/R_s$ = 4 to 6% for a sample with five NiFe layers (Fig. 1), where $\Delta R = R - R_s$ and R_s is the resistance at saturation. The resistance of the as-deposited sample drops about 15% after it anneals at any temperature in the 300° to 400°C range. Thus, changes in ΔR dominate the variation in $\Delta R/R_s$ with annealing temperature. A difference in the magnitudes of the GMR for fields applied parallel and perpendicular to the current direction indicates a persistent anisotropic magnetoresistance (AMR) effect of magnitude 0.3 to 0.5% in both the unannealed and annealed samples. As the anneal temperature increases, the width and hysteresis of $\Delta R/R_s$ versus the applied field H increase. We find a maximum $\Delta R/R_s$ = 5.34% after an anneal at 335°C with a full width at half maximum (FWHM) of 22 Oe, but the sample that was annealed at 315°C shows the largest change in resistance per unit field: $(\Delta R/R_s)$/FWHM = 4% per 5 Oe = 0.8% per oersted. The largest sensitivity that we have observed in similar structures is 3.3% per 2.75 Oe = 1.2% per oersted. To our knowledge this is the largest sensitivity reported in any multilayer or alloy GMR structure.

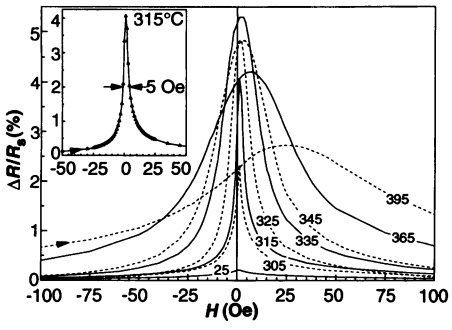

Fig. 1. $\Delta R/R_s$ versus H for Ta(100 Å)-Ag(20 Å)-[NiFe(20 Å)-Ag(40 Å)]$_4$-NiFe(20 Å)-Ag(20 Å)-Ta(40 Å)-SiO_2(700 Å)-Si. Temperatures (in degrees Celsius) are marked on curves. The field is in the plane of the sample and perpendicular to the current. Arrows indicate the ramping direction of the field. Unannealed samples show only a small AMR effect, but for annealing temperatures above 300°C, a large GMR effect is evident. **(Inset)** Large sensitivities of order 0.8% per oersted are achieved in the sample annealed at 315°C.

All samples shown in Fig. 1 show hysteresis in the magnetization with coercivities increasing from 2 Oe for the sample annealed at 315°C to 14 Oe for the sample annealed at 395°C. Also, the distinction between the easy and hard axis directions decreases rapidly with annealing temperature and nearly vanishes at annealing temperatures above 325°C. As annealing temperature is varied, the magnetoresistance becomes larger as the remanence magnetization M_r/M_s becomes smaller (Fig. 2), suggesting that ease of demagnetization plays an important role in the determination of $\Delta R/R_s$. Interestingly, M_r/M_s decreases and $\Delta R/R_s$ increases as the annealing temperature increases to about 345°C, but at higher annealing temperatures, the trend reverses. The sample with 25 Å Ag spacer thickness maintains a smaller $\Delta R/R_s$ and larger M_r/M_s throughout the annealing sequence. Also, samples with 10 Å Ag spacers show no significant GMR before or after annealing.

Unlike the results reported so far in continuous multilayer systems, GMR is evident in the one-layer sample (Fig. 3), although only of magnitude 0.3%, and is clearly distinguishable from the AMR effect because the magnetoresistance is negative for the field both parallel and perpendicular to the current. These samples are roughly consistent with the functional dependence $\Delta R/R_s \sim (n-1)/n$, where n is the number of magnetic layers, implying that the dominant contribution to the GMR comes from the number of NiFe-Ag-NiFe sandwiches.

Cross-sectional transmission electron microscopy (TEM) and x-ray diffraction (XRD) were used to examine the microstructure of the films, which were found to have a strong (111) fiber texture. The TEM results indicate a columnar microstructure with ~200 Å grain size and epitaxy between the NiFe and Ag from layer to layer within a single column. The as-deposited sample has the complex XRD peak pattern expected of a superlattice structure and a low magnetoresistance attributable to AMR (Fig. 4). After the first anneal, at 310°C, the total diffracted intensity increased, presumably because of a reduction in the number of scattering defects in the film and consistent with the observed decrease in resistance. Significantly, this first anneal also shows the appearance of GMR with reduced relative intensity and broadening of the satellite peaks, indicating a deterioration of the quality of the superlattice. The sample annealed at 330°C showed the highest magnetoresistance in this series, 5.6%, and shows further deterioration of the superlattice structure. This deterioration is nearly complete for the sample annealed at 370°C, with a reduced magnetoresistance of 4.0%. The above association of degraded superlattice structure with GMR is supported by TEM (*14*), with which frequent interruptions in the continuity of the NiFe layers by Ag penetration at grain boundaries can be observed.

In the unannealed films, the magnetic layers are continuous and coupled ferromagnetically to adjacent layers and, therefore, have large values of M_r/M_s and do not show GMR. The origin of this coupling may be interlayer exchange, mediated by the Ag spacer, or small "bridges" or "pinholes" of NiFe across the Ag spacer. For samples with very thin Ag spacers, we favor the second explanation, which has been offered previously to explain the ferromagnetic coupling in NiFe-Ag spin-valve structures with thin Ag layers (*15*). The TEM and XRD confirm that a breakup of the magnetic layers is simultaneous with the appearance of GMR. Hence, we expect a multidomain or particle-like magnetic state within each layer. For anneals aggressive enough to promote substantial grain boundary diffusion, we suppose that the domain size will scale roughly with the grain size of the film. Larger domains would be expected in samples in which the degree of magnetic layer breakup is reduced.

Discontinuities induced in the magnetic layers, particularly those arranged into columns such as the grain boundaries in the columnar microstructure reported here, will prompt an interlayer magnetostatic interaction that favors antiparallel order of the moments in adjacent planes. Complete islanding of the grains into individual particles is not required; any reduction in the amount of magnetic flux transported across a grain boundary will result in magnetostatic interactions. In sufficiently discontinuous multilayers, the magnetostatic interac-

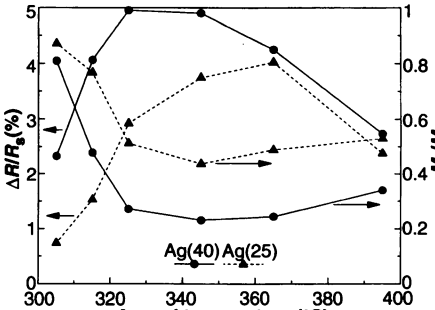

Fig. 2. The amplitude $\Delta R/R_s$ and magnetization squareness M_r/M_s versus annealing temperature for Ta(100 Å)-Ag(20 Å)-[NiFe(20 Å)-Ag(x)]$_4$-NiFe(20 Å)-Ag(20 Å)-Ta(40 Å)-SiO_2(700 Å)-Si, where x = 25 (triangles) and 40 Å (circles). In general, $\Delta R/R_s$ increases with decreasing M_r/M_s. Unannealed samples (not shown) exhibit large $M_r/M_s \sim 0.93$ and no GMR. The 25 Å Ag spacer shows a systematically larger M_r/M_s and smaller $\Delta R/R_s$ than the 40 Å Ag spacer.

tion may dominate any spacer-layer–mediated ferromagnetic exchange that determines the magnetic state of the unannealed multilayer. Also, discontinuous magnetic layers may reduce ferromagnetic interlayer coupling by promoting the isolation of pinholes. The breaking of the ferromagnetic order between layers by magnetostatic interactions or pinhole isolation provides an explanation for the increase in $\Delta R/R_s$ and the decrease in M_r/M_s with increasing anneal temperature (Figs. 1 and 2). The reversal of this trend at the highest annealing temperatures may be the result of severely disrupted magnetic layers that bridge to adjacent layers through the spacer.

We suggest that the structures reported here are sensitive at low fields because we can select the amount of magnetostatic coupling needed to offset the ferromagnetic exchange coupling between layers by the degree of magnetic layer discontinuity afforded by a particular annealing temperature. Depending on the degree of magnetic layer breakup, our estimates indicate that the interlayer magnetostatic interaction energies are easily comparable with the interlayer exchange energies (*15*) in weakly coupled multilayer systems. Hence, in the search for low-field GMR structures, one might select weakly ferromagnetically exchange-coupled or uncoupled multilayer systems and seek to induce a degree of discontinuity in the magnetic layers to produce GMR. Because we expect an inhomogeneous distribution of both the magnetostatic and exchange interactions across the surfaces of a discontinuous, disrupted multilayer, we also expect significant local variations in the relative orientations of moments in adjacent layers, ranging continuously from completely antiparallel to completely parallel, depending on the local interlayer and intralayer interactions. Consistent with this interpretation, although M_r/M_s is greatly reduced as the samples are annealed (Fig. 2), a completely antiparallel state, for which $M_r/M_s = 0$, is not achieved. The smaller $\Delta R/R_s$ and larger M_r/M_s observed in the sample with the 25 versus 40 Å Ag spacer (Fig. 2) might be the result of a greater ferromagnetic exchange coupling between magnetic layers in the sample with the thinner spacer.

Other observations also support the idea of a multidomain or multiparticle, discontinuous multilayer structure. The origin of the GMR in the annealed single layer film is similar to that of the granular alloys: spin-dependent scattering from domain to domain (or particle to particle) within the layer. Larger GMR is observed in multilayered samples for two possible reasons: (i) The active surface area for scattering between adjacent layers is much larger than that for scattering between adjacent particles within a layer, and (ii) magnetostatic interactions between discontinuous layers foster a greater degree of antiparallel alignment of the magnetic moments. The increases in the FWHM and the hysteresis in $\Delta R/R_s$ versus H (Fig. 1) and the decrease in the induced uniaxial anisotropy with annealing temperature are also consistent with a breakup of the magnetic layers. As the magnetic layers become more discontinuous, increased magnetostatic interactions or, alternatively, increased domain wall pinning will increase hysteresis and the field needed to magnetize the sample and mask any induced anisotropy (some deterioration of the anisotropy attributable to decreased pair ordering of the alloy may also occur).

As in our work, Rodmacq *et al.* (*16*) report no GMR in Ni-Ag samples with 10 Å spacers deposited at room temperature because of discontinuities in the Ag spacer. Unlike our results, however, samples of NiFe(12.5 Å)-Ag(10.5 Å) deposited at 100 K showed $\Delta R/R_s = 17\%$ and saturation fields of 300 Oe at room temperature without annealing. After annealing at 280°C for 10 min, these samples showed an increase in sensitivity from 0.056% to 0.165% per oersted, primarily as the result of a large decrease in the saturation field, which the authors attribute to structural changes that modify the interlayer exchange interaction. Annealing above 300°C "destratifies" the layers and degrades the magnetoresistance, presumably because of bridging through the Ag spacer. Interestingly, at nearly the same temperature, we see the onset of GMR in our samples with thick spacers, which we also attribute to a breakup of the layers. Also, although we see similar trends in the GMR with annealing temperature for spacer thicknesses of 20 to 40 Å, these authors report that GMR is strongly peaked at a spacer layer thickness of 11 Å with FWHM = 3.5 Å. These observations suggest a difference in the dominant interlayer coupling mechanism in the two cases, magnetostatic in our case and exchange in theirs. We expect that the magnetostatic interaction in the annealed samples reported by Rodmacq *et al.* (*16*) will be quite small compared with the interlayer exchange interaction because the annealing temperatures reported are low compared with ours and the saturation fields are relatively high.

Two other recent reports also discuss GMR in annealed NiFe-Ag structures. Bian *et al.* (*17*) report large increases in the magnetoresistance at 4.2 K of NiFe(4 Å)-Ag(20 Å) multilayers after annealing for 20 min at temperatures between 300° and 600°C. After an anneal at 450°C, individual particles of order 60 to 100 Å in size were observed. Saturation fields as small as 50 Oe with a corresponding $\Delta R/R_s = 8\%$ are reported at 4.2 K. Sensitivities at room temperature are not indicated, but one might expect superparamagnetism for the samples with small particle sizes (*11*). Kitada (*18*) has recently reported a large increase in the magnetoresistance of NiFe-Ag bilayer thin films after successively an-

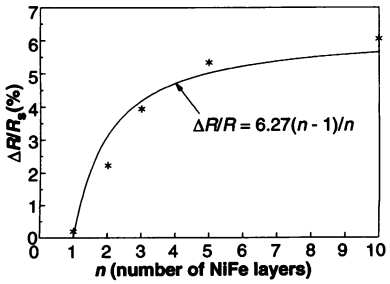

Fig. 3. $\Delta R/R_s$ versus n, the number of NiFe layers, for Ta(100 Å)-Ag(20 Å)-[NiFe(20 Å)-Ag(40 Å)]$_{n-1}$-NiFe(20 Å)-Ag(20 Å)-Ta(40 Å)-SiO_2(700 Å)-Si annealed to yield the maximum value of $\Delta R/R_s$. The increase in $\Delta R/R_s$ with number of layers suggests that the GMR is primarily a multilayer effect. However, a small $\Delta R/R$ is also observed in the one-layer sample.

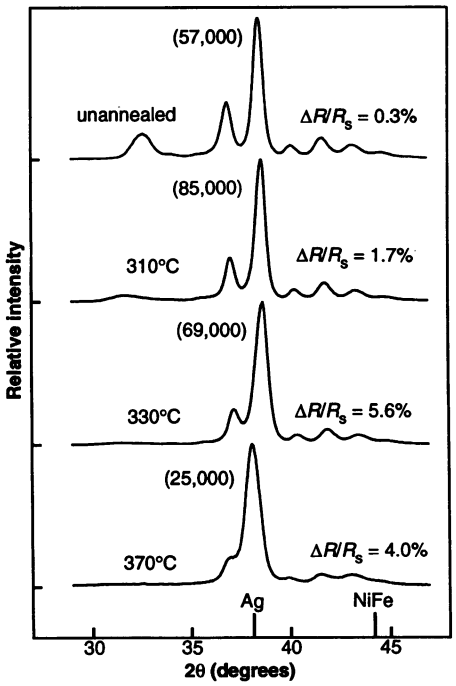

Fig. 4. Normalized high-angle XRD patterns and magnetoresistance values for the same sample structure as in Fig. 1 in the as-deposited condition and after annealing for 10 min at different temperatures. The numbers in parentheses indicate the intensity (in numbers of counts) of the major peak for each scan, and the tick marks at 38.150° and 44.166° indicate the positions of the (111) bulk Ag and NiFe peaks, respectively. The complex satellite peak structure of the as-deposited superlattice monotonically degrades with annealing, whereas a maximum GMR value of 5.6% is observed for an intermediate anneal temperature.

nealing the films in oxygen and then hydrogen for 5 min at 300°C. He reports $\Delta R/R_s$ = 5.6% for characteristic fields of about 30 Oe at room temperature and speculates that the thermal processing promotes first a mixing of the NiFe and Ag layers followed by precipitation of Ag within the NiFe.

REFERENCES

1. M. N. Baibich, J. M. Broto, A. Fert, F. Nguyen Van Dau, F. Petroff, *Phys. Rev. Lett.* **61**, 2472 (1988).
2. G. Binasch, P. Grunberg, F. Saurenbach, W. Zinn, *Phys. Rev. B* **39**, 4828 (1989).
3. S. S. P. Parkin, N. More, K. P. Roche, *Phys. Rev. Lett.* **64**, 2304 (1990).
4. B. Dieny *et al.*, *Phys. Rev. B* **43**, 1297 (1991).
5. J. Q. Xiao, J. S. Jiang, C. L. Chien, *Phys. Rev. Lett.* **68**, 3749 (1992).
6. A. E. Berkowitz *et al.*, *ibid.*, p. 3745.
7. J. A. Barnard *et al.*, *J. Magn. Magn. Mater.* **114**, L230 (1992).
8. C. Dupas *et al.*, *J. Appl. Phys.* **67**, 5680 (1990).
9. T. Shinjo and H. Yamamato, *J. Phys. Soc. Jpn.* **59**, 3061 (1990).
10. S. S. P. Parkin, *Phys. Rev. Lett.* **67**, 3598 (1991).
11. T. L. Hylton, *Appl. Phys. Lett.* **62**, 2431 (1993).
12. M. A. Parker, K. R. Coffey, T. L. Hylton, J. K. Howard, *Mater. Res. Soc. Symp. Proc.*, in press.
13. K. R. Coffey, T. L. Hylton, M. A. Parker, J. K. Howard, *Appl. Phys. Lett.*, in press.
14. M. A. Parker, T. L. Hylton, K. R. Coffey, J. K. Howard, in preparation.
15. B. Dieny *et al.*, *J. Appl. Phys.* **69**, 4774 (1991).
16. B. Rodmacq, G. Palumbo, Ph. Gerard, *J. Magn. Magn. Mater.* **118**, L11 (1993).
17. X. Bian *et al.*, *Mater. Res. Soc. Symp. Proc.*, in press.
18. M. Kitada, *J. Magn. Magn. Mater.* **123**, L18 (1993).

17 May 1993; accepted 7 July 1993

Hydrogen in Stishovite, with Implications for Mantle Water Content

Alison R. Pawley,* Paul F. McMillan, John R. Holloway

Stishovite, the highest pressure polymorph of silicon dioxide, may be an important mineral in some regions of the Earth's mantle. Fourier transform infrared spectroscopy has been used to determine the hydrogen content of synthetic stishovite. The concentration of hydrogen depends on the aluminum content of the sample and reaches a maximum of 549 ± 23 hydrogen atoms per 10^6 silicon atoms for an Al_2O_3 content of 1.51 percent by weight. Stishovite could be a storage site for water in deep subducting slabs and in regions of the mantle that are too hot for hydrous minerals to be stable.

The presence of even trace amounts of water in the Earth's mantle has a major effect on its rheology, seismicity, phase equilibria, and melting behavior. Recent studies have shown that significant amounts of hydrogen can be contained in nominally anhydrous upper mantle minerals such as pyroxene, garnet, and rutile (*1–3*). In addition, β-Mg_2SiO_4, likely a major component of the transition zone (410 to 660 km deep), has been synthesized with H in its structure (*4*). Stishovite is the highest pressure polymorph of SiO_2. It is abundant in silica-rich regions of the mantle at depths greater than about 300 km, including subduction zones, which are sites at which water is returned to the Earth's interior. We have investigated whether H can be incorporated in stishovite by using polarized Fourier transform infrared (FTIR) spectroscopy and secondary ion mass spectrometry (SIMS) to determine H content and speciation and the site of H incorporation in the stishovite structure.

It has been postulated that the manner in which H substitutes into stishovite is similar to the way it substitutes into rutile (TiO_2) (*3, 5*), with which stishovite is isostructural. Stishovite has a tetragonal structure (Fig. 1A), with Si in sixfold coordination and chains of edge-sharing octahedra extending along the *z* axis. Polarized infrared (IR) spectroscopy of rutile has shown that the OH-stretching absorption is strongly pleochroic; intensity is greatest when the electric vector of the IR radiation is perpendicular to the *c* axis of the crystal. This result indicates that the OH dipole is oriented perpendicular to *c*. A neutron diffraction study of H-containing rutile indicated that the position of the H on the (001) plane is displaced slightly from the midpoint of the shared O-O edge of the TiO_6 octahedron (*3*).

We prepared eight samples of stishovite containing H_2O and D_2O at 10 GPa and 1200°C in a Walker-style multianvil device (*6*). Samples 1, 3, and 4 (H-stishovite) and sample 2 (D-stishovite) contain only minor impurities (Table 1) and are coarse-grained and prismatic (Fig. 1B). However, the stishovite crystals synthesized from Al-bearing bulk compositions 5 to 7 (Al-stishovite) contain more than 1% Al_2O_3 by weight; they are fine-grained and many are twinned (Fig. 1C).

We obtained single crystal IR absorption spectra using micro-FTIR techniques (*7*). The unpolarized spectrum of H-stishovite (Fig. 2A) shows a sharp absorption at 3111 cm^{-1} and two weak absorptions at 3240 and 3311 cm^{-1}; the absorptions are caused by OH-stretching vibrations. In the polarized spectra (Fig. 2B), the greatest absorption of the 3111-cm^{-1} band occurs when the electric vector of the IR radiation is polarized perpendicular to *c*, and there is no absorbance when it is polarized parallel to *c*. Of the minor peaks, the more intense one at 3311 cm^{-1} is also polarized, whereas the 3240-cm^{-1} feature appears to have the same intensity for all orientations, although in many spectra it cannot be distinguished from the background noise. The spectrum of D-stishovite (Fig. 2C) contains a

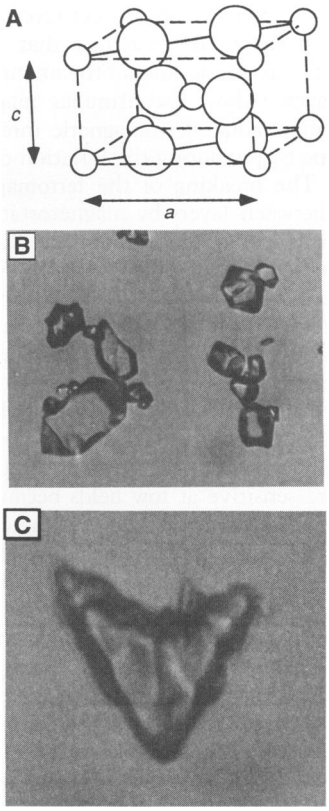

Fig. 1. Stishovite structure and morphology. (**A**) Structure: small circles represent silicon atoms and large circles represent oxygen atoms. (**B**) Prismatic crystals typical of stishovite crystallized in SiO_2-H_2O/D_2O experiments. The largest crystal shown is 25 μm wide; the maximum crystal length in these samples is 1 mm. (**C**) Twinned crystal typical of stishovite crystallized in SiO_2-Al_2O_3-H_2O experiments. The longest edge length is 22 μm and the twin plane is at an angle of 26° to *c*. The maximum crystal size in these samples is 100 μm. All samples also contain acicular stishovite up to 100 μm long and thin platelets of coesite up to 200 μm long. Both minerals are more abundant in the samples with higher H_2O content and so are interpreted to have crystallized from a SiO_2-rich fluid on temperature quench. In all samples, stishovite is recognized by its high refractive index (n_ω = 1.799 and n_ϵ = 1.826) and high birefringence (δ = 0.027).

A. R. Pawley and P. F. McMillan, Department of Chemistry, Arizona State University, Tempe, AZ 85287.
J. R. Holloway, Departments of Chemistry and Geology, Arizona State University, Tempe, AZ 85287.
*To whom correspondence should be addressed.